PHYSICAL REVIEW B **92**, 041407(R) (2015)

Controlling the electronic structure of graphene using surface-adsorbate interactions

Piotr Matyba,[1,*] Adra Carr,[1] Cong Chen,[1] David L. Miller,[2] Guowen Peng,[3] Stefan Mathias,[4,5] Manos Mavrikakis,[3] Daniel S. Dessau,[1] Mark W. Keller,[2] Henry C. Kapteyn,[1] and Margaret Murnane[1]

[1]*Department of Physics and JILA, University of Colorado and NIST, Boulder, Colorado 80309, USA*

[2]*National Institute of Standards and Technology (NIST), 325 Broadway, Boulder, Colorado 80305, USA*

[3]*Department of Chemical and Biological Engineering, University of Wisconsin-Madison, Madison 53706, USA*

[4]*Department of Physics and Research Center OPTIMAS, University of Kaiserslautern, 67663 Kaiserslautern, Germany*

[5]*Physikalisches Institut, Georg-August-Universität Göttingen, Friedrich-Hund-Platz 1, 37077 Göttingen, Germany*

(Received 18 December 2014; revised manuscript received 3 May 2015; published 21 July 2015)

Hybridization of atomic orbitals in graphene on Ni(111) opens up a large energy gap of ≈2.8 eV between nonhybridized states at the K point. Here we use alkali-metal adsorbate to reduce and even eliminate this energy gap, and also identify a new mechanism responsible for decoupling graphene from the Ni substrate without intercalation of atomic species underneath. Using angle-resolved photoemission spectroscopy and density functional theory calculations, we show that the energy gap is reduced to 1.3 eV due to moderate decoupling after adsorption of Na on top of graphene. Calculations confirm that after adsorption of Na, graphene bonding to Ni is much weaker due to a reduced overlap of atomic orbitals, which results from n doping of graphene. Finally, we show that the energy gap is eliminated by strong decoupling resulting in a quasifreestanding graphene, which is achieved by subsequent intercalation of the Na underneath graphene. The ability to partially decouple graphene from a Ni substrate via n doping, with or without intercalation, suggests that the graphene-to-substrate interaction could be controlled dynamically.

DOI: 10.1103/PhysRevB.92.041407 PACS number(s): 73.22.Pr, 68.65.Pq, 68.43.Jk, 74.25.Jb

Graphene features unique optical and electronic properties that promise utilization in novel optoelectronic devices [1–4]. These properties originate in the conical dispersion of states near the K point of the Brillouin zone, which form a Dirac cone and are degenerate at the Fermi level [1]. These states change in response to atoms adsorbed on top of graphene (doping) or when coupling to the substrate is strong. In the case of graphene on metals, the energy of the Dirac cone can change as a result of interfacial doping, or a band gap can open up at the K point when the symmetry of the lattice is broken [5–9].

Graphene can be grown on commensurate metal surfaces by decomposition of gaseous precursors [10]. Although this method is very efficient and yields large-area graphene, the strong coupling to the substrate and doping change the band structure near the K point [5]. Coupling to the substrate is exceptionally strong for graphene on Ni(111) [Gr/Ni(111)], where the overlap of atomic orbitals from graphene and the substrate leads to hybridization. As a result, the π state mixes with the substrate d band, forming a manifold of states spanning the energy from 0 to 3 eV below the Fermi level [5,11–13]. Although some of these states intersect at the K point and feature a similar structure to the Dirac cone, utilization of Gr/Ni(111) in devices requires decoupling from the substrate [14,15].

Intercalation of atomic species into Gr/Ni(111) was shown to decouple the substrate by forming an atomic spacer [11–13,16]. Although this method is used to produce quasifreestanding graphene for spectroscopy, the mechanisms of this decoupling are not entirely understood. Noble metals were shown to restore the Dirac cone after intercalation [12,17]. However, studies of alkali-metal intercalants have resulted in severe inconsistencies. On the one hand, intercalation of Na (and similarly K or Cs) was postulated to restore the Dirac cone incompletely, and reduce the energy gap between the nonhybridized states at the K point (the π-to-π^* energy gap) from 2.8 to 1.3 eV [16,18]. On the other hand, angle-resolved photoemission spectroscopy (ARPES) and density functional theory (DFT) showed that the Dirac cone is restored completely and the energy gap reduced to 0 eV after intercalation [15]. The origins of the large 1.3 eV energy gap found in previous experiments, as well as the observed inconsistencies between different studies, are not understood. We note that adsorption of alkali metals on top of graphene induce n doping and was used to control the electronic structure of bilayers of graphene on SiC(0001) [19]. Mechanisms of alkali metals intercalation of graphene were also studied using DFT and scanning tunneling microscopy (STM) [20–25].

In this Rapid Communication, we use ARPES to probe the dispersion of states near the K point during adsorption and subsequent intercalation of atomic Na into Gr/Ni(111). The dispersion of states is a sensitive probe of coupling between graphene and the substrate [12,26] that allows us to observe two distinct regimes of decoupling that were not observed previously. First, we find that Na on top of graphene induces a moderate decoupling from the substrate that is evident from partial restoration of the Dirac cone, which increases the dispersion of the π state at high momenta and decreases the π-to-π^* energy gap from 2.8 to 1.3 eV. This decoupling was previously misinterpreted as due to intercalation of atomic Na (and K or Cs) into Gr/Ni(111) [16,18]. Second, we find that proper intercalation of the Na underneath graphene induces a much stronger decoupling, which is evident from a restoration of the pristine Dirac cone at the K point (i.e., the π-to-π^* energy gap is reduced to ≈0 eV). Our experimental findings are confirmed by DFT band structure calculations and Bader charge analysis.

*piotr.matyba@jila.colorado.edu

Ni(111) single crystal films were graphitized in UHV through dissociation of C_2H_4 under partial pressure of 10^{-6} Torr and Ni temperature of 900 K [10]. This monolayer of graphite was dissolved then into Ni(111) at temperatures >1100 K and subsequently precipitated onto the surface by slow cooling. The solubility of C in Ni is three times higher at 1100 K than at room temperature [27], making it possible to control the formation of graphene on the surface by cooling the sample [28]. Gr/Ni(111) formed at lower rates ($\approx$2 h per monolayer), through precipitation of carbon rather than by direct dissociation of C_2H_4, showed the much better morphology that was critical for this study. Na was adsorbed under a pressure of $\approx 10^{-10}$ Torr at room temperature using a commercial Na source. Intercalation of Na was induced by annealing the sample at temperatures in the range of 300–450 K, followed by rapid cooling to room temperature [29].

ARPES was performed using 40.8 eV vacuum ultraviolet radiation from a He discharge lamp (Specs UVS300) and a hemispherical analyzer (Specs Phoibos 100). The morphology of Gr/Ni(111) was examined using ARPES and low-energy electron diffraction (LEED). Intercalation of Na was diagnosed through exposures to O_2 in UHV, which results in oxidation of Na when on top of graphene but not intercalated (due to the large size of the O_2 molecule [30]). DFT calculations were performed using the VASP code [31] based on spin-polarized DFT [29]. The projector augmented wave potentials were used to model electron-ion interactions [32,33] and van der Waals (vdW) dispersion forces were accounted for using the vdW-DF approach [31,34–36].

The band structure of Gr/Ni(111), measured experimentally along the ΓK [12,13,16] and p-ΓK [14,15] directions of the Brillouin zone, revealed that coupling to the substrate distorts the states near the K point. In Fig. 1(a) we plot this band structure probed along the ΓK direction. The exact position

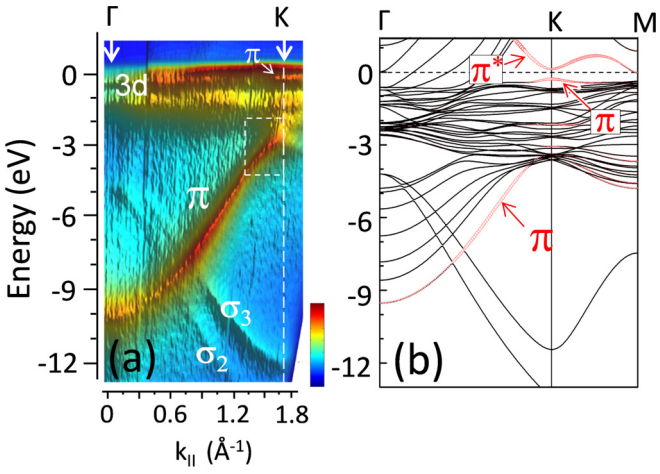

FIG. 1. (Color online) (a) Electronic structure of pristine Gr/Ni(111) measured along the ΓK direction in the Brillouin zone; the π, σ_2, and σ_3 states of graphene and the 3d band of Ni(111) are indicated with symbols, while high symmetry points of the Brillouin zone (Γ,K) are indicated with vertical white arrows. (b) Calculated majority band structure of Gr/Ni(111). The graphene $2p_z$ contributions are highlighted in red (thick lines).

of the K point is established from the minimum of the σ_3 state, and the position of the Γ point from the minimum of the π state. For the π state, we find that the maximum is lower in energy by $\approx$2.8 eV compared to graphene on SiC(0001) and the minimum is lower by $\approx$2.0 eV. These two energy offsets at Γ and K, which are not equal, indicate that the state dispersion (dE/dk) along ΓK must be lower in Gr/Ni(111) than in graphene on SiC(0001).

Indeed, the experimental spectrum in Fig. 1(a) shows that the π state dispersion is lower in the momentum range from 1.4 to 1.7 Å^{-1} (indicated in the figure). We attribute this dispersion lowering to the coupling between the π state and d band in the corresponding momentum range. In order to gain further insights into this coupling, we performed DFT calculations of the most stable (top-fcc) configuration, shown in Fig. 1(b). Our calculations omit the spectral weights and matrix elements relevant for ARPES, making it possible to show all of the important states along the ΓK direction (note that the experimental spectrum is dominated by the strongest spectral features). We find that the Ni d band spans from the Fermi level down to -3.5 eV along the entire cut through the Brillouin zone and near the Γ point from -5 to -9 eV, as shown in Fig. 1(b). These higher binding energy states near Γ are not accessible in ARPES due to matrix element effects and can be neglected in our analysis [14].

Importantly, our calculations show that the d band and π state hybridize near the K point and split into a manifold of states [5,14–16]. The spectral intensity of this manifold is low along the ΓK direction due to matrix element effects induced by hybridization [37–39], but it was probed previously using higher energy photons and/or other cuts through the Brillouin zone [14,15]. The lowering of the π state dispersion in the momentum range from 1.4 to 1.7 Å^{-1} in Fig. 1(b) is directly caused by the hybridization. We note that the lower density of Ni states near the Fermi level causes hybridization to be weaker, and remnants of the π state are seen near the K point in Figs. 1(b) and 1(a), and also in Fig. S1(b) [29].

Our DFT calculations show that the π^* state is shifted in energy to above the Fermi level and its dispersion is nonlinear near the K point, in Fig. 1(b). We link this peculiar dispersion to the same hybridization that changes the π state below the Fermi level and we anticipate that the π^* state will shift in response to n doping when Na is on top of Gr/Ni(111).

Indeed, with 0.8 monolayer of Na on top, the π^* state is slightly populated and below the Fermi level in Fig. 2(b). However, changes in the π state after adsorption cannot be explained as due to n doping. That state maximum shows up at energy higher than before adsorption and the dispersion is higher near the K point, which results in a lower π-to-π^* energy gap. Since n doping should neither shift a populated state towards the Fermi level nor change the state dispersion, we conclude that adsorption of Na reduced the coupling between graphene and the substrate, and thus the π-to-π^* energy gap decreased from 2.8 to 1.3 eV. Before we validate this interpretation through theory below, we emphasize that the π state is hybridized above -2.8 eV before adsorption in Fig. 2(a) and it is not hybridized after adsorption in Fig. 2(b).

Graphene can be decoupled from the substrate either when the adsorbate is intercalated underneath graphene to form an

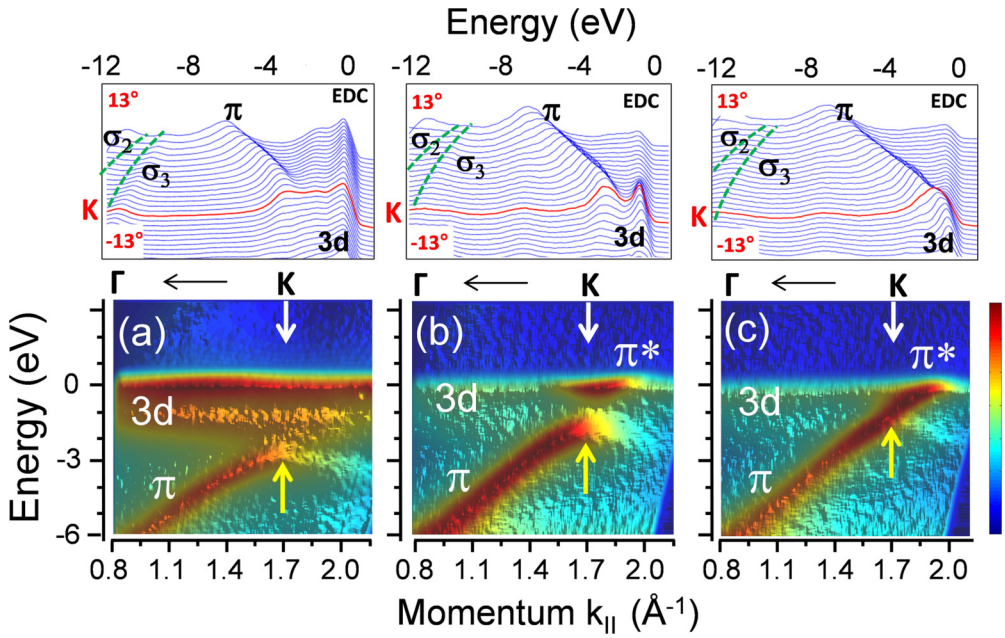

FIG. 2. (Color online) (a) Experimental band structure of graphene on Ni(111), where the K point is indicated by vertical white arrows (↓). The insets above show the energy distribution curves (EDCs) near the K point [the K-point EDC is indicated in red (thick line)] as a function of detection angle. The EDCs energy range is from −12 to 1 eV. (b) Same as (a) but after adsorption of 0.8 monolayer Na on top; the minimum of the π^* state is visible at the Fermi level. The yellow vertical arrows (↑) indicate roughly the maximum of the π state, established from the state turning point. (c) Same as (b) after further annealing to intercalate Na to underneath graphene.

atomic spacer separating the substrate, or when the adsorbate resides on top and induces a weakening of the graphene-to-substrate (π-d) bond. We excluded intercalation as the origin of decoupling in Fig. 2(b), by exposing samples to O_2 inside the UHV chamber. The photoemission lines from sodium oxides, which can be formed when Na is on top of graphene, indicated that Na was on top after adsorption [29]. We also exclude intercalation at isolated areas that would produce partially decoupled graphene. Previous ARPES studies of Na intercalation into Gr/Ni(111) [15] showed that partial intercalation results in a superposition of two π states, one from intercalated and another from unintercalated graphene. Since such superposition is not seen in our measurements, we conclude that all Na remains on top of Gr/Ni(111) in Fig. 2(b).

In order to understand the mechanism of this decoupling in Fig. 2(b), we compare the calculated band structures of Gr/Ni(111) before and after adsorption, in Figs. 3(b) and 3(c), respectively (energy is referenced to the Fermi level to allow the comparison). Before adsorption, the π^* state is above and the remnant of the π state is below the Fermi level. After adsorption, these two states are shifted in energy vs the Fermi level in agreement with our experimental results in Fig. 2(b). We emphasize that all states should be shifted correspondingly because the work function is lower after adsorption. However, states below the Fermi level (except for the remnants of the π state) remain at the same energy as before adsorption. Since the spectral intensity of these states is strongly diminished [40] and the π state is partially unhybridized [see Fig. 2(b)], we conclude that charge rearrangements after adsorption screen the coupling between graphene and the substrate and cause lowering the π-to-π^* energy gap. We also note that weak hybridization still persists although the coupling between graphene and the substrate is firmly attenuated. Therefore, since the spectral intensities are not included in the calculations, changes to the band structures induced by adsorption of Na on top [in Fig. 3(c)] are very subtle when compared to the experimental spectrum in Fig. 2(b). We anticipate that including the intensity into the calculations would reflect the decoupling; and this deserves further theoretical investigation.

Importantly, we can observe the decoupling by analyzing Bader charge distributions before and after adsorption [in Fig. 4(a)] and structural changes to Gr/Ni(111) [in Fig. 4(b)]. Before adsorption, the atomic orbitals of graphene (p_z) and Ni(111) ($3d_{3z^2-r^2}$) overlap and give rise to a covalentlike (π-d) bond and the charge density redistribution shown in Fig. 4(a). Bader charge shows that a net charge of 0.10e (e is the elementary charge) is transferred from the substrate to graphene. After adsorption, the charge redistribution and the associated energetics shift due to electrons supplied by the adsorbate. Bader charge shows that Na brings a net charge of 0.36e per atom to graphene and virtually no charge to the substrate. This charge supplied to graphene induces an interfacial dipole that can lower its propensity of bonding to the substrate, as evidenced from lifting graphene up to 2.30 Å above the substrate in Fig. 4(b). Our DFT calculations show that the net charge transferred to graphene drops to 0.05e per atom, indicating a weaker overlap of the p_z and $3d_{3z^2-r^2}$ orbitals after adsorption. We conclude that the observed decoupling may result from a dynamic competition between the π-d and d-d hybridization, which favors weaker coupling to the substrate after adsorption. We anticipate that a higher charge transfer per atom from the adsorbate would yield even stronger decoupling, which is consistent with previous measurements on Gr/Ni(111) [16,18].

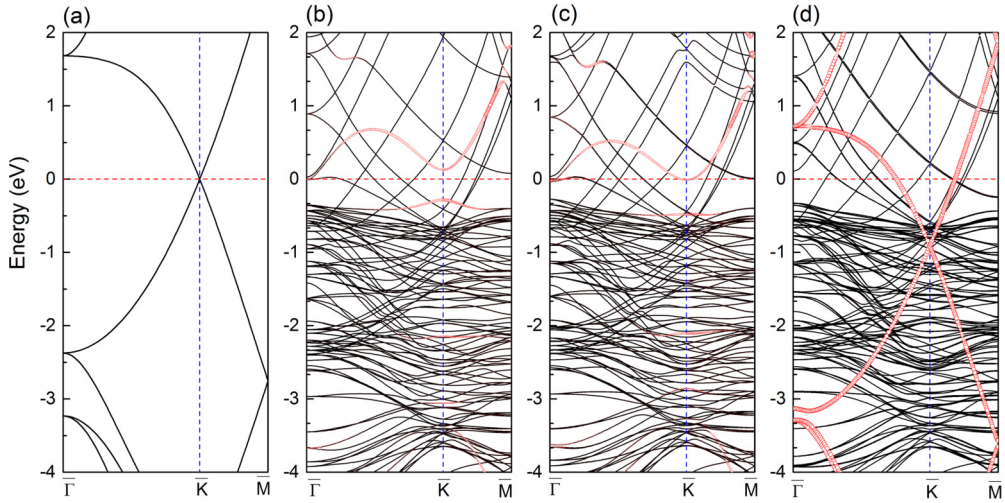

FIG. 3. (Color online) Band structures for (a) freestanding graphene, (b) Gr/Ni(111), (c) Na/Gr/Ni(111), and (d) Gr/Na/Ni(111) in a (2×2) supercell, corresponding to a Na coverage of 0.75 ML. The contributions of graphene $2p_z$ orbitals are highlighted in red (thick line) in panels (b)–(d).

We emphasize that decoupling of graphene from Ni when Na is on top is different from decoupling due to noble metal atoms intercalated into Gr/Ni(111), which was investigated in past work [8,9,11,12,30]. Atoms intercalated into Gr/Ni(111) break down hybridization, cleave the π-d bond, and detach graphene from the substrate. Electron-donating adsorbates (such as Na) on top of graphene cause decoupling by weakening the π-d bond, but in this case graphene is not detached from the substrate.

We confirm our interpretation of the different degrees of decoupling due to Na on top or underneath graphene by forcing the intercalation of Na into Gr/Ni(111), shown in Fig. 2(c). In order to allow a direct comparison, this study was performed with the sample fixed in front of the detector [29]. After intercalation, the π-to-π^* energy gap is closed and the Dirac cone is restored near the K point. The remnant gap opening ($<$100 meV) and minor band back-bending observed in Fig. 2(c) result from superposition of regions with different concentrations of the intercalated Na. This is reasonable due to the supply of Na and bottlenecks in the intercalation paths. The results of DFT calculations shown in Figs. 3(d) and 4(c) show that graphene is lifted up to 4.9 Å above the substrate. We conclude that intercalation of Na causes identical decoupling as intercalation of noble metals, while adsorption on top causes only a moderate decoupling and lowering the π-to-π^* energy gap to 1.3 eV.

Previous observations of lowering the π-to-π^* energy gap from 2.8 to 1.3 eV were interpreted as due to decoupling the substrate by intercalation of Na (and K or Cs) into Gr/Ni(111) [16,18], but no evidence of intercalation was shown. We emphasize that angle-resolved or angle-integrated x-ray photoelectron spectroscopy (XPS) measurements cannot confirm intercalation because changes in the intensity of XPS lines from a monolayer of Na (K,Cs) adsorbed on Gr/Ni(111) are often caused by formation of thick islands of adsorbates on top rather than intercalation [22,30,41,42]. Our measurements provide strong evidence that Na on top of Gr/Ni(111) reduces coupling between graphene and the substrate, and

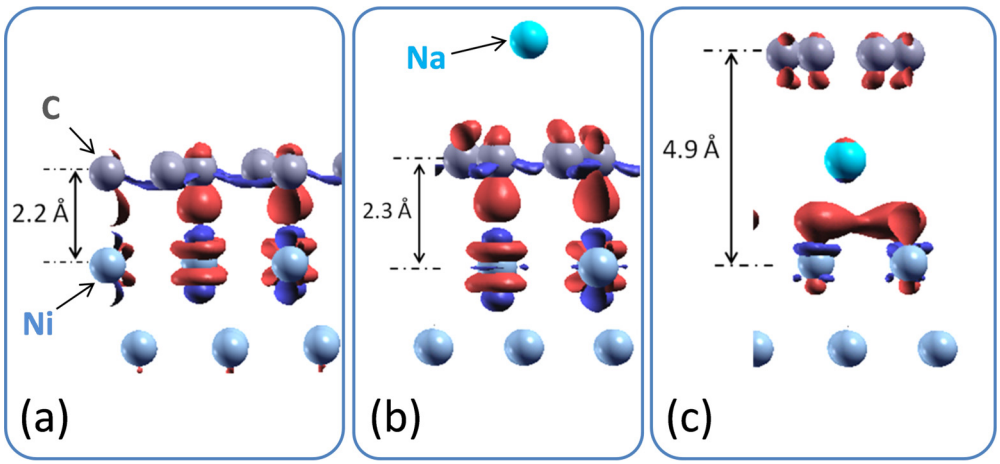

FIG. 4. (Color online) Charge density difference plots, using an isosurface of $\pm 0.02\, e/\text{Å}^3$ for (a) Gr/Ni(111), (b) Na/Gr/Ni(111), and (c) Gr/Na/Ni(111); charge density accumulation is shown in red and depletion in blue. The adsorption energy of Na on Gr/Ni is -1.00 eV at a Na coverage of 1 ML, referenced to the total energies of atomic Na and Gr/Ni(111).

causes lowering of the π-to-π^* energy gap from 2.8 to 1.3 eV.

Although recent experiments suggested that Na may intercalate spontaneously due to the low-energy barrier [15,43], we do not observe spontaneous intercalation at room temperature. Instead, we find that intercalation is not possible unless graphene features defects and/or grain boundaries (which is expected owing to the size of atomic Na) and unless the mobility of Na is increased at high temperature. Our DFT calculations further support this observation—although the arrangement with Na on top is not optimal from the energetics standpoint and the adsorbate tends to intercalate, the intercalation is kinetically limited without grain boundaries and defects in graphene.

In order to corroborate the above argumentation, we performed intercalation studies on Gr/Ni(111) grown under different conditions. We were able to achieve good control over the concentration of defects in graphene, by introducing oxide impurities into the Ni(111) substrate and by performing the growth at lower temperatures producing impurities of amorphous carbon [44,45]. Our study shows that intercalation of Na depends on morphology of Gr/Ni(111). When graphene displays relatively weak spectral features in ARPES and LEED, with a high background of secondary electrons, intercalation is possible at lower temperatures. Intercalation into a higher quality graphene requires elevated temperature and intercalation into the highest quality graphene needs temperatures close to the desorption threshold.

Our observations show that adsorption of Na at temperatures lower than room temperature reduces the π-to-π^* energy gap to less than 1.3 eV in some cases, which we link to the nature of Na overlayers and/or graphene-Na interaction at low temperatures. Adsorption at low temperatures causes aggregation of Na, while adsorption at higher temperatures causes adatoms to be mobile and dispersed randomly on the surface [41,46,47]. This is consistent with our observations that poor morphology of Na on top causes a weaker decoupling, and might explain a recent observation that adsorption at 133 K does not induce major changes to the band structure of Gr/Ni(111) [15]. We anticipate that aggregation of the Na on top may cause a lower net charge transfer to graphene and a different competition between the π-d and d-d hybridizations, thus causing weaker decoupling. Detailed understanding of this effect would require additional studies using STM or XPS.

In summary, we show that the presence of Na atoms on top of Gr/Ni(111) induce decoupling of graphene from the substrate, as evident from a decrease of the π-to-π^* energy gap to 1.3 eV. Moreover, intercalation of Na underneath graphene recovers near-pristine graphene, closing this energy gap to near 0 eV. We anticipate that the mechanism of controlling the extent of graphene-to-substrate coupling using a charge transfer from adsorbates (rather than intercalation) opens new possibilities in using optical (laser) excitations to control this coupling in graphene on other surfaces. This technique might allow for switching the graphene-to-substrate coupling in the spirit of previous work on noble metal surfaces and alkali-metal adsorbates (cf. Refs. [48,49]).

The authors gratefully acknowledge support from the National Science Foundation Physics Frontiers Center Program and the Moore Foundation. D.D. acknowledges support from DOE-BES Grant No. DE-FG02-03ER46066. P.M. acknowledges a fellowship from the Swedish Research Council (Vetenskapsrådet, No. 623-2011-935). Work at the University of Wisconsin was partially supported by Department of Energy-Basic Energy Sciences (DOE-BES) and by the Air Force Office of Scientific Research under Basic Research Initiative AFOSR Grant No. FA9550-12-1-0481. The computational work was performed in part using supercomputing resources from the following institutions: EMSL, a National scientific user facility at Pacific Northwest National Laboratory (PNNL); the Center for Nanoscale Materials (CNM) at Argonne National Laboratory (ANL); and the National Energy Research Scientific Computing Center (NERSC). EMSL is sponsored by the Department of Energy's Office of Biological and Environmental Research located at PNNL. CNM and NERSC are supported by the U.S. Department of Energy, Office of Science, under Contracts No. DE-AC02-06CH11357 and No. DE-AC02-05CH11231, respectively.

Equipment is identified in this Rapid Communication only in order to adequately specify the experimental procedure. Such identification does not imply endorsement by the National Institute of Standards and Technology (NIST), nor does it imply that the equipment identified is the best available for the purpose.

[1] A. K. Geim and K. S. Novoselov, Nat. Mater. **6**, 183 (2007).
[2] K. Zou, X. Hong, and J. Zhu, Phys. Rev. B **84**, 085408 (2011).
[3] K. S. Novoselov, A. K. Geim, S. V. Morozov, D. Jiang, M. I. Katsnelson, I. V. Grigorieva, S. V. Dubonos, and A. A. Firsov, Nature (London) **438**, 197 (2005).
[4] K. I. Bolotin, K. J. Sikes, Z. Jiang, M. Klima, G. Fudenberg, J. Hone, P. Kim, and H. L. Stormer, Solid State Commun. **146**, 351 (2008).
[5] E. Voloshina and Y. Dedkov, Phys. Chem. Chem. Phys. **14**, 13502 (2012).
[6] M. Papagno, S. Rusponi, P. M. Sheverdyaeva, S. Vlaic, M. Etzkorn, D. Pacile, P. Moras, C. Carbone, and H. Brune, ACS Nano **6**, 199 (2012).
[7] A. L. Walter, S. Nie, A. Bostwick, K. S. Kim, L. Moreschini, Y. J. Chang, D. Innocenti, K. Horn, K. F. McCarty, and E. Rotenberg, Phys. Rev. B **84**, 195443 (2011).
[8] M. Amft, S. Lebegue, O. Eriksson, and N. V. Skorodumova, J. Phys.: Condens. Matter **23**, 395001 (2011).
[9] Y. J. Ren, S. S. Chen, W. W. Cai, Y. W. Zhu, C. F. Zhu, and R. S. Ruoff, Appl. Phys. Lett. **97**, 053107 (2010).

[10] D. L. Miller, M. W. Keller, J. M. Shaw, A. N. Chiaramonti, and R. R. Keller, J. Appl. Phys. **112**, 064317 (2012).
[11] A. Varykhalov, J. Sanchez-Barriga, A. M. Shikin, C. Biswas, E. Vescovo, A. Rybkin, D. Marchenko, and O. Rader, Phys. Rev. Lett. **101**, 066804 (2008).
[12] A. Varykhalov, M. R. Scholz, T. K. Kim, and O. Rader, Phys. Rev. B **82**, 121101 (2010).
[13] D. Haberer *et al.*, Nano Lett. **10**, 3360 (2010).
[14] A. Varykhalov, D. Marchenko, J. Sanchez-Barriga, M. R. Scholz, B. Verberck, B. Trauzettel, T. O. Wehling, C. Carbone, and O. Rader, Phys. Rev. X **2**, 041017 (2012).
[15] Y. S. Park, J. H. Park, H. N. Hwang, T. S. Laishram, K. S. Kim, M. H. Kang, and C. C. Hwang, Phys. Rev. X **4**, 031016 (2014).
[16] A. Gruneis and D. V. Vyalikh, Phys. Rev. B **77**, 193401 (2008).
[17] A. Reina, X. T. Jia, J. Ho, D. Nezich, H. B. Son, V. Bulovic, M. S. Dresselhaus, and J. Kong, Nano Lett. **9**, 30 (2009).
[18] A. Nagashima, N. Tejima, and C. Oshima, Phys. Rev. B **50**, 17487 (1994).
[19] T. Ohta, A. Bostwick, T. Seyller, K. Horn, and E. Rotenberg, Science **313**, 951 (2006).
[20] M. Petrović *et al.*, Nat. Commun. **4**, 2772 (2013).
[21] D. V. Chakarov, L. Osterlund, B. Hellsing, V. P. Zhdanov, and B. Kasemo, Surf. Sci. **311**, L724 (1994).
[22] S. Watcharinyanon, L. I. Johansson, C. Xia, and C. Virojanadara, J. Appl. Phys. **111**, 083711 (2012).
[23] D. W. Boukhvalov and C. Virojanadara, Nanoscale **4**, 1749 (2012).
[24] Y. C. Li, G. Zhou, J. Li, J. Wu, B. L. Gu, and W. H. Duan, J. Phys. Chem. C **115**, 23992 (2011).
[25] S. M. Choi and S. H. Jhi, Appl. Phys. Lett. **94**, 153108 (2009).
[26] C. Hwang, D. A. Siegel, S. K. Mo, W. Regan, A. Ismach, Y. G. Zhang, A. Zettl, and A. Lanzara, Sci. Rep. **2**, 590 (2012).
[27] W. W. Dunn, R. B. McLellan, and W. A. Oates, Trans. Metall. Soc. AIME **242**, 2129 (1968).
[28] Y. Zhang, L. Zhang, and C. Zhou, Acc. Chem. Res. **46**, 2329 (2013).
[29] See Supplemental Material at http://link.aps.org/supplemental/10.1103/PhysRevB.92.041407 for details of sample preparation, Na intercalation, and DFT calculations.
[30] Y. S. Dedkov, M. Fonin, U. Rudiger, and C. Laubschat, Appl. Phys. Lett. **93**, 022509 (2008).
[31] G. Kresse and J. Furthmüller, Phys. Rev. B **54**, 11169 (1996).
[32] P. E. Blochl, Phys. Rev. B **50**, 17953 (1994).
[33] G. Kresse and D. Joubert, Phys. Rev. B **59**, 1758 (1999).
[34] M. Dion, H. Rydberg, E. Schroder, D. C. Langreth, and B. I. Lundqvist, Phys. Rev. Lett. **92**, 246401 (2004).
[35] J. Klimeš, D. R. Bowler, and A. Michaelides, J. Phys.: Condens. Matter **22**, 022201 (2010).
[36] J. Klimeš, D. R. Bowler, and A. Michaelides, Phys. Rev. B **83**, 195131 (2011).
[37] M. Mulazzi, M. Hochstrasser, M. Corso, I. Vobornik, J. Fujii, J. Osterwalder, J. Henk, and G. Rossi, Phys. Rev. B **74**, 035118 (2006).
[38] T. Haarlammert, L. Bignardi, C. Winter, G. Fecher, P. Rudolf, and H. Zacharias, Eur. Phys. J. B **86**, 225 (2013).
[39] S. Hüfner, *Photoelectron Spectroscopy: Principles and Applications* (Springer-Verlag, Berlin, 1995).
[40] A submonolayer of adsorbate should not diminish significantly the spectral intensity of the underlying layer.
[41] M. Breitholtz, T. Kihlgren, S. A. Lindgren, H. Olin, E. Wahlstrom, and L. Wallden, Phys. Rev. B **64**, 073301 (2001).
[42] M. Breitholtz, T. Kihlgren, S. A. Lindgren, and L. Wallden, Phys. Rev. B **67**, 235416 (2003).
[43] I.-Y. Jeon *et al.*, Sci. Rep. **3**, 1810 (2013).
[44] F. Mittendorfer, A. Garhofer, J. Redinger, J. Klimeš, J. Harl, and G. Kresse, Phys. Rev. B **84**, 201401(R) (2011).
[45] Y. Gamo, A. Nagashima, M. Wakabayashi, M. Terai, and C. Oshima, Surf. Sci. **374**, 61 (1997).
[46] C. G. Hwang, S. Y. Shin, S.-M. Choi, N. D. Kim, S. H. Uhm, H. S. Kim, C. C. Hwang, D. Y. Noh, S.-H. Jhi, and J. W. Chung, Phys. Rev. B **79**, 115439 (2009).
[47] A. Sandin, T. Jayasekera, J. E. Rowe, K. W. Kim, M. B. Nardelli, and D. B. Dougherty, Phys. Rev. B **85**, 125410 (2012).
[48] H. Petek, M. J. Weida, H. Nagano, and S. Ogawa, Science **288**, 1402 (2000).
[49] H. Petek, M. J. Weida, H. Nagano, and S. Ogawa, Surf. Sci. **451**, 22 (2000).